

Helicity separation in heavy-ion collisions

Mircea Baznat^{*} and Konstantin Gudima[†]

*Joint Institute for Nuclear Research, 141980 Dubna (Moscow region), Russia
and Institute of Applied Physics, Academy of Sciences of Moldova, MD-2028 Kishinev, Moldova*

Alexander Sorin[‡] and Oleg Teryaev[§]

*Joint Institute for Nuclear Research, 141980 Dubna (Moscow region), Russia
and Dubna International University, Dubna (Moscow region) 141980, Russia*

(Received 22 March 2013; revised manuscript received 23 October 2013; published 13 December 2013)

We study the P -odd effects related to the vorticity of the medium formed in noncentral heavy-ion collisions. Using the kinetic quark-gluon strings model, we perform numerical simulations of the vorticity and hydrodynamical helicity for various atomic numbers, energies, and centralities. We observed vortical structures typically occupy the relatively small fraction of the fireball volume. In the course of numerical simulations, the noticeable hydrodynamical helicity was observed to manifest specific mirror behavior with respect to the reaction plane. The effect is maximal at the Nuclotron based Ion Collider fAcility and Facility for Antiproton and Ion Research in Europe energy range.

DOI: [10.1103/PhysRevC.88.061901](https://doi.org/10.1103/PhysRevC.88.061901)

PACS number(s): 25.75.-q

Introduction. The local violation [1] of discrete symmetries in strongly interacting QCD matter is now under intensive theoretical and experimental investigation. The renowned chiral magnetic effect (CME) uses the $C(P)$ -violating (electro)magnetic field emerging in heavy-ion collisions in order to probe the $(C)P$ -odd effects in QCD matter.

There is an interesting counterpart of this effect, chiral vortical effect (CVE) [2], that is due to the coupling to P -odd medium vorticity. In its original form [2] this effect leads to the appearance of the same electromagnetic current as CME. Its straightforward generalization was proposed to result in generation of all conserved-charge currents [3], in particular baryonic ones (especially important when there is CME cancellation among three massless flavors [4]), and polarization of hyperons [3,5]. Let us also mention a recent theoretical development [6], the discovery of a remarkable relation to gravitational anomalies.

The key problem is whether the flows developing in heavy-ion collisions possess vorticity. This is especially interesting as vorticity is a universal phenomenon manifested at very different scales of macro and micro physics. One can observe it in spiral galaxies, cyclones and typhoons, semiconductors, chemical reactions, biological systems, quantum field theories, etc. It would be very important to push this concept further to the internal structure of QCD matter.

The noncentral heavy-ion collisions could naturally generate a rotation (global or local, both related to vorticity) with an angular velocity normal to the reaction plane, which is their generic qualitative feature. However, finding proper quantitative characteristics of these phenomena requires special investigation [7,8]. In this paper we address this problem using the quark-gluon strings model (QGSM) and observe the

clear signs and manifestations of vortical and helical structures in QCD matter formed in noncentral heavy-ion collisions. In particular, we observed the novel effect of the hydrodynamical helicity separation.

Modeling velocity, vorticity, and helicity in kinetic model. One of the first models designed to describe the dynamics of energetic heavy-ion collisions was the intranuclear cascade model developed in Dubna [9] which is based on the Monte Carlo solution of a set of the Boltzmann-Uehling-Uhlenbeck relativistic kinetic equations with collision terms, including cascade-cascade interactions. For particle energies below 1 GeV it is sufficient to consider only nucleons, pions, and Δ s. The model includes a proper description of pion and baryon dynamics for particle production and absorption processes. In the original version the nuclear potential is treated dynamically, i.e., for the initial state it is determined using the Thomas-Fermi approximation, but later on its depth is changed according to the number of knocked-out nucleons. This allows one to account for nuclear binding. The Pauli principle is implemented by introducing a Fermi distribution of nucleon momenta as well as Pauli blocking factors for scattered nucleons.

At energies higher than about 10 GeV, the quark-gluon string model (QGSM) is used to describe elementary hadron collisions [10,11]. This model is based on the $1/N_c$ expansion of the amplitude for binary processes where N_c is the number of quark colors. Different terms of the $1/N_c$ expansion correspond to different diagrams, which are classified according to their topological properties. Every diagram defines how many strings are created in a hadronic collision and which quark-antiquark or quark-diquark pairs form these strings. The relative contributions of different diagrams can be estimated within Regge theory, and all QGSM parameters for hadron-hadron collisions were fixed from the analysis of experimental data. The breakup of strings via creation of quark-antiquark and diquark-antidiquark pairs is described by the Field-Feynman method [12], using phenomenological functions for the fragmentation of quarks, antiquarks, and diquarks into hadrons. The modified non-Markovian relativistic

^{*}baznat@theor.jinr.ru

[†]gudima@theor.jinr.ru

[‡]sorin@theor.jinr.ru

[§]teryayev@theor.jinr.ru

kinetic equation, having a structure close to the Boltzmann-Uehling-Uhlenbeck kinetic equation but accounting for the finite formation time of newly created hadrons, is used for simulations of relativistic nuclear collisions. One should note that QGSM considers the two lowest SU(3) multiplets in mesonic, baryonic, and antibaryonic sectors, so interactions between almost 70 hadron species are treated on the same footing. This is a great advantage of this approach and is important for the proper evaluation of the hadron abundances and characteristics of the excited residual nuclei. The energy extremes were bridged by the QGSM extension downward in the beam energy [13].

For investigation of dynamical formation of velocity \vec{v} and vorticity $\vec{\omega}$ ($\equiv \text{rot } \vec{v}$) fields in relativistic heavy-ion collision, the coordinate space was divided into $50 \times 50 \times 100$ cells of volume $dx dy dz$ with $dx = dy = 0.6$ fm, $dz = 0.6/\gamma$ fm, where γ is the Lorentz factor of equal velocity system of collision. In this reference system the total momentum and total energy of the produced particles were calculated in all cells for each of fixed 25 moments of time t covering the interval of 10 fm/c.

The results were averaged for about 10 000 heavy-ion collisions with identical initial conditions. The spectator nucleons of projectile or target ions, which at given time momentum do not undergo any individual collision, were included in evaluation of velocity. The velocity field in the given cell was defined by the following double sum over the particles in the cell and over the all simulated collisions:

$$\vec{v}(x, y, z, t) = \frac{\sum_i \sum_j \vec{P}_{ij}}{\sum_i \sum_j E_{ij}}, \quad (1)$$

where \vec{P}_{ij} and E_{ij} are the momentum and energy of particle i in the collision j , respectively. The vorticity was calculated using discrete partial derivatives.

We paid special attention to the pseudoscalar characteristics of the vorticity, that is, the hydrodynamical helicity $H \equiv \int dV (\vec{v} \cdot \vec{\omega})$, which is related to a number of interesting phenomena in hydrodynamics and plasma physics, such as the turbulent dynamo (providing a possible additional mechanism of magnetic field generation on the later stages of heavy-ion collisions) and Lagrangian chaos. It might be compared the analog of topological charge $Q = \int d^3x J^0(x)$, where the current $J^\mu = \epsilon^{\mu\nu\rho\gamma} u_\nu \partial_\rho u_\gamma$ [as usual, the four-velocity $u_\nu \equiv \gamma(1, \vec{v})$] contributes to the hydrodynamical anomaly [14] and the polarization of hyperons [3,5]. The calculation of the topological charge, which is the correct relativistic generalization of the hydrodynamical helicity, leads to the extra factor γ^2 in the integrand. Still, as the helicity itself is a more traditional quantity, we use it for the numerical calculations.

Results of the simulations: Helicity separation effect. The averaged (over 10 000 events) qualitative pictures of velocity and vorticity fields corresponding to Au + Au collisions at $\sqrt{s_{NN}} = 5$ GeV with the impact parameter 8 fm equal to the (transverse) radius of the nuclei are presented in Figs. 1 and 2.

Figure 1 represents the three-dimensional distribution (top) of the velocity defined by the collision participants and produced particles after 10 fm/c of the evolution and its

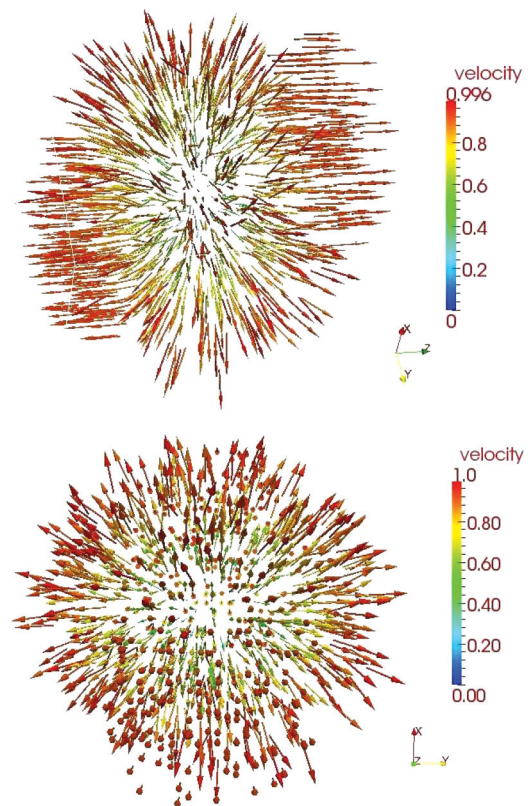


FIG. 1. (Color online) Three-dimensional image (top) and projection on plane xy (bottom) of velocity field in Au + Au at $\sqrt{s_{NN}} = 5$ GeV, $b = 8$ fm, and $t = 10$ fm/c.

projection (bottom) to the transverse xy plane. The direction, length, and color of the arrows represent the direction and size of the velocity. We clearly see the picture of a little bang when the fastest particles (pions) occupy the most distant positions from the collision origin.

Figure 2 shows the similar distributions for the vorticity. The vorticity is concentrated in the relatively thin ($2 \div 3$ fm) layer at the boundary of the participant region. This might be an analog of the vortex sheet expected when Kelvin-Helmholtz instability develops [15]. Let us stress that in the case under consideration it emerges in the kinetic approach, which might be of some interest for the microscopic description of turbulence.

For quantitative description of this phenomena, we use the hydrodynamic helicity whose patterns are presented in Figs. 3 and 4.

Figure 3 shows the helicities in Au + Au collisions at different impact parameters evaluated in different domains. One can see that the helicity calculated with inclusion of the all cells is zero (black line). For the cells with the definite sign of the velocity components, which are orthogonal to the reaction plane (which may be selected also experimentally), the helicity is nonzero and changes sign for the different signs of these components (red and blue lines, respectively; color online only). The effect is growing with impact parameter and represents a sort of saturation in time.

This effect of helicity separation is one of our main results. Let us stress that the calculation in the hybrid Ultrarelativistic

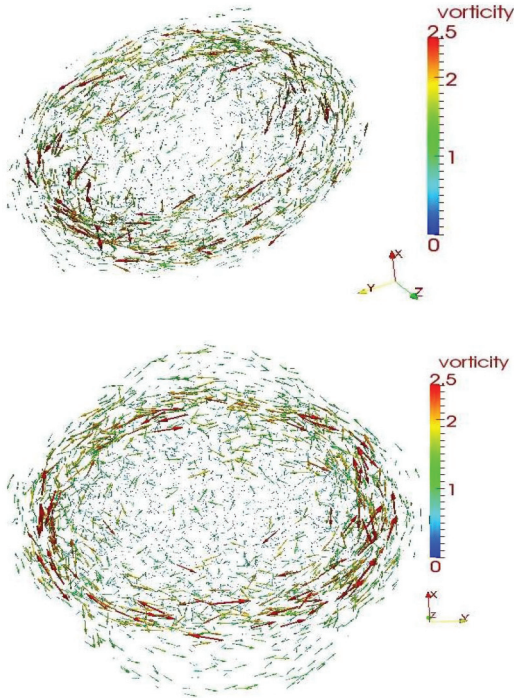


FIG. 2. (Color online) Three-dimensional image (top) and projection on plane xy (bottom) of vorticity field in Au + Au at $\sqrt{s_{NN}} = 5$ GeV, $b = 8$ fm, and $t = 10$ fm/c.

Quantum Molecular Dynamics model manifests very similar behavior [16]. This is not surprising as the helicity is in fact generated at the hydrodynamical stage of the model, while the transition from kinetic to hydrodynamical stage should be performed similarly to that done in Eq. (1).

This effect might be qualitatively explained, if the perpendicular components of velocities (which are selected to have different signs) and the corresponding vorticities (assumed to have the same signs) provide the dominant contribution to the scalar product in the helicity definition. However, the numerical analysis showed [see Fig. 3(b)] that the longitudinal components along the beam directions (z axis) provide even larger contribution to the helicity than contributions from the transverse direction (y axis). Note that comparable values of z

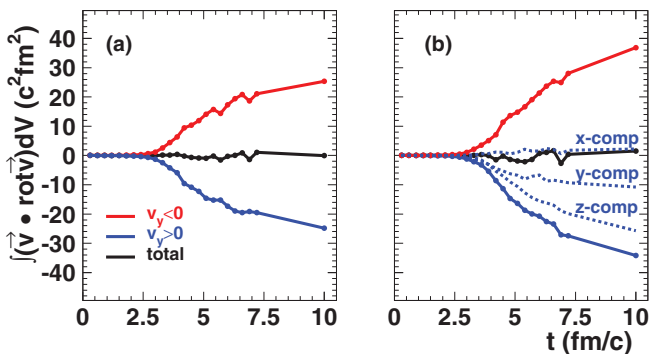


FIG. 3. (Color online) Time dependence of integrated helicity in Au + Au at $s^{1/2} = 5$ GeV at different impact parameters; $b = 4$ fm for (a) and $b = 8$ fm for (b), where the contributions of various components of vorticity and velocity are also shown.

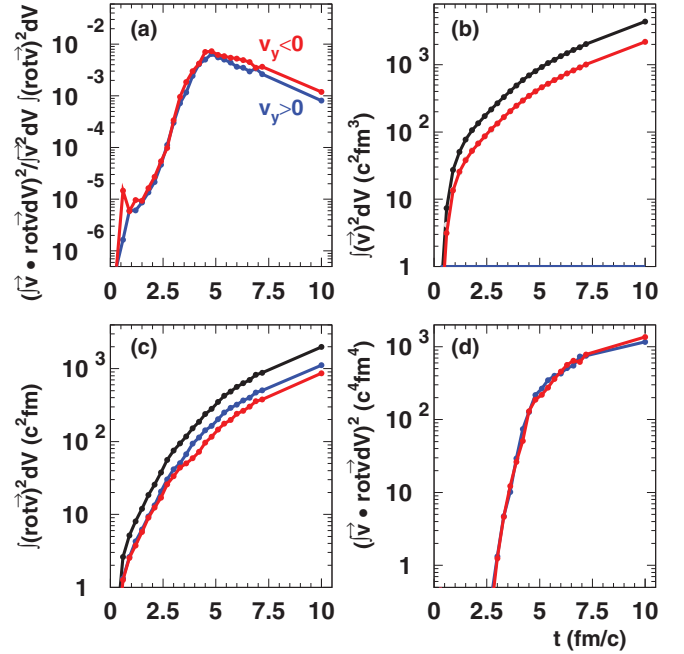


FIG. 4. (Color online) Time dependence of Cauchy-Schwarz bound for helicity in Au + Au at $s^{1/2} = 5$ GeV at impact parameter $b = 8$ fm(a); the integrated squares of velocity (b), vorticity (c), and helicity (d).

and y components to helicity is due to larger z components of velocity and y components of vorticity.

So, such a qualitative picture is oversimplified, but it still provides the correct sign convention for the helicity-separation effect.

The energy dependence of the helicity-separation effect appears to be very weak, with the maximal value achieved around the Nuclotron based Ion Collider fAcility (NICA) energy range.

It is instructive to clarify the roles played by velocity and vorticity in forming the helicity. Figure 4 shows the dimensionless ratio bounded from above by 1 due to Cauchy-Schwarz inequality as well its dimensionful ingredients. This bound is saturated for helical flows with vorticities parallel to velocities. In the case of incompressible fluids the helicity of such flows is proportional to the (nonrelativistic) kinetic energy. The actual values of this ratio show that the correlation between the directions of the vorticity and the velocity is not large but is non-negligible. Let us estimate whether the generated helicity should be sufficient to provide the hyperon polarization effect mentioned above.

Helicity and polarization of hyperons. The hydrodynamical helicity should give rise to the polarization of Λ hyperons with the sign differing for the particles with “up” and “down” y components of their momenta, so that the hyperons acquire the helicity in the course of their motion transverse to the reaction plane. As we already suggested earlier [3], the effect is pronounced at moderate (NICA) energies due to large (strange) chemical potential. The current investigation shows that, luckily, the helicity at these energies is also noticeable.

For semiquantitative estimate of this effect one may use the average strange chiral charge produced by the zeroth

component of the respective current

$$Q_5^s = \frac{N_c}{2\pi^2} \int d^3x \mu^2(x) \epsilon^{ijk} u_i \partial_j u_k = \frac{\langle \mu^2 \rangle N_c H}{2\pi^2},$$

where we use the mean value theorem to extract the value of the square of strange chemical potential at some point inside the integration region and get the helicity from the remaining integral. Assuming that the strange chirality is carried by the Λ hyperons whose average number in each event is $\langle N_\Lambda \rangle$ one get the estimate for its average polarization as

$$\langle P_\Lambda \rangle \sim \frac{\langle \mu^2 \rangle N_c H}{2\pi^2 \langle N_\Lambda \rangle}.$$

For numerical estimate at NICA energies, we take (see Fig. 3) $H = 30 \text{ fm}^2 (c = 1)$ and, as typical values, $\langle \mu^2 \rangle = 900 \text{ MeV}^2$, $\langle N_\Lambda \rangle = 15$ to get $\langle P_\Lambda \rangle \sim 0.8\%$. This value is not large but does not exclude the opportunity to measure the effect. Note that it is indirectly supporting the actual calculations of helicity as the obtained expression respects the density matrix positivity [17] limit $P_\Lambda \leq 1$. Should the helicity be much larger (resulting in the appearance of a much larger value of the dimensionless ratio plotted in Fig. 4), a much larger number of hyperons (and/or K^* mesons) would be required to preserve the density matrix positivity. This is an example of the situation when the spin-dependent effects may be used [17] to bound the spin-averaged cross sections from below.

Of course, more detailed calculations of polarization taking into account the spatial distribution of chemical potential and the kinematics of produced hyperons will be required.

Conclusions and outlook. We investigated vorticity and hydrodynamical helicity in noncentral heavy-ion collisions in the framework of the kinetic quark-gluon string model. We have observed that the vorticity is predominantly localized in a relatively thin layer ($2 \div 3 \text{ fm}$) on the boundary

between the participant and spectator nucleons. This might be qualitatively understood in the spirit of the core-corona type models [18,19].

Thus, the gradients of the velocities in the region occupied by the participants are small due to the compensation of momenta between the target and projectile particles in the c.m. frame. As a result, the vorticity is substantial only in the thin transition layer between the participant (i.e., core) and the spectator (i.e., corona) regions. We found the novel effect of the helicity separation in heavy-ion collisions when it has different signs below and above of the reaction plane. We have investigated its dependence on the type of nuclei and collision energy and observed that it is maximal in the NICA energy range. We have also calculated the degree of alignment of the velocity and vorticity which is maximal for the Beltrami flows, whose relativistic generalization is currently under investigation [20].

We used the obtained values of helicity for estimates of Λ hyperon polarization in heavy-ion collisions at NICA energy range due to previously suggested [3] mechanism. The resulting polarization is about 1% and may be studied experimentally. Of course, more detailed theoretical investigations are required.

In particular, the discovery of an extra T^2 term [6] raises again the question of why polarization was not observed at RHIC. Here one may refer to the (exponential) dilution of polarization by temperature effects (similar to what happens at a much larger scale in polarized targets), although this problem certainly requires further investigation.

Acknowledgments. We are indebted to E. L. Bratkovskaya, K. A. Bugaev, L. Csernai, V. D. Kekelidze, K. Landsteiner, V. D. Toneev, V. Voronyuk, V. I. Zakharov, G. M. Zinovjev, and especially M. Bleicher, J. Steinheimer, and H. Stöcker for useful discussions and comments. This work was supported in part by the Russian Foundation for Basic Research, Grant No. 11-02-01538-a.

-
- [1] K. Fukushima, D. E. Kharzeev, and H. J. Warringa, *Phys. Rev. D* **78**, 074033 (2008).
- [2] D. Kharzeev and A. Zhitnitsky, *Nucl. Phys. A* **797**, 67 (2007).
- [3] O. V. Rogachevsky, A. S. Sorin, and O. V. Teryaev, *Phys. Rev. C* **82**, 054910 (2010).
- [4] D. E. Kharzeev and D. T. Son, *Phys. Rev. Lett.* **106**, 062301 (2011).
- [5] J.-H. Gao, Z.-T. Liang, S. Pu, Q. Wang, and X.-N. Wang, *Phys. Rev. Lett.* **109**, 232301 (2012).
- [6] K. Landsteiner, E. Megias, L. Melgar, and F. Pena-Benitez, *J. High Energy Phys.* **09** (2011) 121.
- [7] F. Becattini and L. Tinti, *Ann. Phys.* **325**, 1566 (2010).
- [8] B. Betz, M. Gyulassy, and G. Torrieri, *Phys. Rev. C* **76**, 044901 (2007).
- [9] V. D. Toneev and K. K. Gudima, *Nucl. Phys. A* **400**, 173C (1983).
- [10] V. D. Toneev, N. S. Amelin, K. K. Gudima, and S. Yu. Sivoklov, *Nucl. Phys. A* **519**, 463C (1990).
- [11] N. S. Amelin, E. F. Staubo, L. P. Csernai, V. D. Toneev, and K. K. Gudima, *Phys. Rev. C* **44**, 1541 (1991).
- [12] R. D. Field and R. P. Feynman, *Nucl. Phys. B* **136**, 1 (1978).
- [13] N. S. Amelin, K. K. Gudima, S. Yu. Sivoklov, and V. D. Toneev, *Sov. J. Nucl. Phys.* **52**, 272 (1990).
- [14] D. T. Son and P. Surowka, *Phys. Rev. Lett.* **103**, 191601 (2009).
- [15] L. P. Csernai, D. D. Strottman, and C. Anderlik, *Phys. Rev. C* **85**, 054901 (2012).
- [16] J. Steinheimer (private communication).
- [17] X. Artru, M. Elchikh, J.-M. Richard, J. Soffer, and O. V. Teryaev, *Phys. Rept.* **470**, 1 (2009).
- [18] J. Aichelin and K. Werner, [aXiv:0810.4465](https://arxiv.org/abs/0810.4465)[nucl-th].
- [19] J. Steinheimer and M. Bleicher, *Phys. Rev. C* **84**, 024905 (2011).
- [20] A. S. Sorin and O. V. Teryaev (unpublished).